N95- 33267

19951268 46

# THE EFFECTS OF $CO_2$ ON THE NEGATIVE REACTANT IONS OF IMS

**Glenn E. Spangler**[1]
Environmental Technologies Group, Inc., 1400 Taylor Ave., Baltimore, MD 21284-9840

## ABSTRACT

In the presence of $CO_2$, the negative reactant ions of ion mobility spectrometry (IMS) are ion clusters of $CO_4^-$ and $CO_3^-$. Methyl salicylate is ionized by the $CO_4^-(H_2O)_n(N_2)_m$ reactant ions, but not by the $CO_3^-(H_2O)_n(N_2)_m$ reactant ions. While the $CO_4^-$ ions are formed by direct association, the $CO_3^-$ ions require additional energy to be formed. The additional energy is provided by either excited neutral gas molecules in a metastable state or UV radiation.

## INTRODUCTION

The effects of $CO_2$ on the composition of the negative reactant ions has been the subject of various investigations throughout the history of ion mobility spectrometry (IMS). The investigations started when Spangler and Collins added $CO_2$ to the carrier gas and noted an increase in the drift time for the negative reactant ion.[1] Then as Herbert Hill and his group began to couple supercritical fluid chromatography to IMS, the drift times for several straight-chain methyl ethers were investigated using $CO_2$ for both the carrier and drift gases.[2] While ion drift times were considerably longer, separation of both reactant and product ions was possible using normal operating temperatures for the IMS. More recently, Hayhurst et al. studied the composition of the negative reactant ions using IMS/MS and, similar to Spangler and Carrico, found contributions from $CO_2$.[3,4] The $CO_2$ can enter the system either through an improperly activated 13X scrubber used to precondition the carrier and drift gases or by permeating through a membrane inlet (or other opening) exposed to ambient air. Until now, there has been no indication that $CO_2$ affects significantly the ionization capabilities of IMS. In fact, a wide range of electronegative compounds can be ionized without adverse affects from $CO_2$.

This changed, however, when ETG, Inc. began to investigate non-radioactive ionization sources for IMS. During these investigations, it was found that certain compounds could be negatively ionized using a conventional $^{63}Ni$ ionization source, but not using a nonradioactive ionization source. For example, previous investigators reported the ionization of methyl salicylate to form $(M+O_2)^-$ product ions in the presence of a $^{63}Ni$ radioactive source, but this was not possible using a photoionization source.[5,6] When it was further discovered that methyl salicylate could not be ionized using argon for the carrier and drift gases, the mass spectrometer studies described in this paper were undertaken to investigate causes.

## EXPERIMENTAL METHODS

The investigations were conducted using an IMS/MS system described previously in the open literature.[4] Improvements to the system included replacing the stacked-ring IMS cell with an all-ceramic IMS cell, upgrading the quadrupole mass spectrometer to an EXTREL C50 quadrupole mass spectrometer,[7] and installing a

---

[1]Current Address: 1209 Malbay Drive, Lutherville, MD 21093.

turbomolecular pump in place of the 4-inch diffusion pump. These are shown in Figure 1. Since the flexible design of the new IMS cell was key to the success of the studies, it will be described in more detail.

The IMS cell was assembled on a base-plate which also served as a mounting flange when the cell was coupled to the mass spectrometer. Structurally, the cell was modular in design consisting of three parts:

- Reactor (approx. 2 cm long, 2.5 cm internal diameter, 1.16 megohm resistance)
- Drift Tube (11.4 cm long, 3.8 cm internal diameter, 11.08 megohm resistance)
- Membrane Inlet (OV-101 impregnated microporous Teflon membrane, 1.3 $cm^2$ area)[8]

The cell was attached to the base-plate using four support rods over which the three sections of the cell were slipped. Teflon sheet or ceramic tape impregnated with OV-17 silicone oil pneumatically sealed and electrically insulated the various sections. The assembly was compressed with nuts threaded on the four support rods. The reactor and drift tubes were conductive inlaid tubes (CITs) coated internally with thick film resistor ink and terminated with thick film conductive ink.[9] The cell was biased by attaching electrical leads to the conductive ink pads.

Two ionization sources were used for ionization: a $^{63}Ni$ radioactive source and a photoionization flashlamp. These were implemented by replacing the reactor section of the cell: one reactor containing the $^{63}Ni$ ionization source and the other containing the photoionization source as shown in Figure 1. The second reactor could also be assembled including a radioactive source so that the photoionization lamp irradiated the ions produced by the $^{63}Ni$ radioactive source. The radioactive source was a cylindrical ring of $^{63}Ni$ foil, approximately one inch in diameter and one centimeter long, mounted axially in the reactor.[10] It had a source strength of 15 millicuries and was mounted in a cup which also served as an ion repeller. The source cup was mechanically constrained within the ceramic reactor using "C"-rings which also made electrical contact with the thick film resistor fired on the inner surface of the drift tube. The photoionization source was an EG&G FK-1064 flashlamp (filled with 2 atm. krypton and sealed with a $MgF_2$ window) mounted perpendicular to the axis of the reactor.[11] The lamp was powered with an EG&G PS350 power supply through a FYD-507 lite pak. The flash rate for the flashlamp was controlled using a pulser assembled from a timer chip and optoisolators.

The shutter grid for the IMS cell was a parallel plane grid constructed from photoetched mesh purchased from Buckbee Mears.[12] This grid was deactivated during the experiments and biased to continuously conduct ion current. Since the ion current was measured using the electronics of the mass spectrometer, there was no ion collector.

The temperature of the IMS was measured using four thermocouples placed in contact with the pinhole mounted on the vacuum flange leading into the mass spectrometer, around the drift tube of the IMS halfway between the shutter grid and the mass spectrometer, and in contact with the reactor and membrane inlet of the IMS. Using strategically located heater tapes, the temperatures at these four locations were continuously monitored and automatically controlled with temperature controllers. Thermal gradients were minimized by preheating the carrier and drift gases before they entered the cell.

Purified air or argon (Matheson UN 1006)[13] was used for the carrier, drift and sample gases of the cell. The purified air was generated using a Balston $CO_2$ remover.[14] Before being introduced into the cell, both gases were passed through activated 13X molecular sieve scrubbers.[15] For some of the data, the 13X molecular sieve scrubbers were activated with a purging flow of prepurified nitrogen at 200 °C for 24 hours and for other of the data (including all of the argon data), the 13X molecular sieve scrubbers were activated with a purging flow of prepurified nitrogen at 300 °C for 24 hours. The water content of the gases was monitored using a DuPont 703

phosphorous pentoxide hygrometer[16] which indicated that the purified air contained 0.1 (est.) to 1.5 ppm water when the 13X scrubbers were activated at 300 °C and 2 to 4 ppm when the 13X scrubbers were activated at 200 °C. The argon contained 1.5 to 1.6 ppm water. The water content increased within these ranges as the scrubbers aged. Since the drift gas flowed between the mounting flange for the IMS and the vacuum flange for the mass spectrometer, it also served as a curtain gas for the pinhole. After flowing through a membrane inlet, the carrier gas entered the IMS cell near the shutter grid and exhausted with the drift gas through the reactor (i.e., unidirectional flow).

The $CO_2$ was Airgas syphon type $CO_2$ used without further purification.[17] The methyl salicylate was generated using reagent grade methyl salicylate in a diffusion tube standards generator. The generator was calibrated gravimetrically by periodically weighing the diffusion tube.

The remainder of the operating conditions for the mass spectrometer are given in Table 1.

TABLE 1: Operating Conditions for the IMS/MS

| PARAMETER | | VALUE |
|---|---|---|
| Pressures | Mass Spectrometer | $2.6 \times 10^{-6}$ Torr |
| | Focussing Lenses | $1.8 \times 10^{-4}$ Torr |
| Voltages | Reaction Region Hi Drift | - 2471 Volts (- 1549 Volts w Argon) |
| | Region Hi | - 1922 Volts (- 1000 Volts w Argon) |
| | Aperture Grid | - 129 Volts (- 67 Volts w Argon) |
| | Pinhole | Ground |
| | Focussing Lens #1 | + 44.3 Volts |
| | Focussing Lens #2 | + 17.5 Volts |
| | Focussing Lens #3 | + 80.2 Volts |
| | Focussing Lens #4 | + 30.4 Volts |
| | Focussing Lens #5 | + 45.0 Volts |
| | Pole Zero | + 8.5 to - 1.5 Volts |
| Temperatures | Membrane Inlet | 48 °C |
| | Reaction Region | 45 °C |
| | Drift Region | 54 °C |
| | Pinhole | 53 °C |
| | Mass Spectrometer | Unheated |
| Gas Flows | Carrier Gas | 210 cc/min |
| | Drift Gas | 336 cc/min |
| | Sample Gas | 240 cc/min |

## RESULTS

Using the radioactive source for ionization and purified air for the carrier, drift and sample gases, Figures 2 and 3 show mass spectra for the negative reactant ions and methyl salicylate for two qualities of the purified air. The methyl salicylate was introduced by challenging the membrane inlet with 0.02 - 0.03 mg/m$^3$ methyl salicylate in purified air. While the purified air was passed through a 13X scrubber activated at 200 °C in both

instances, the data of Figure 2 were collected immediately (within several hours) after the scrubber was removed from the oven and reinstalled into the carrier/drift gas flow lines and the data of Figure 3 were collected after the 13X scrubber had aged for several days. The ions with masses 50, 60, 68, 78, 86, 88, 96 and 106 in Figure 2 are $O_2^-(H_2O)_n(N_2)_m$, n = 0 to 2 and m = 0 to 2 overlaying $CO_3^-(H_2O)_n(N_2)_m$, n = 0 to 2 and m = 0 to 1; the ions with masses 82, 100, 110, 128 and 138 are $O_4^-(H_2O)_n(N_2)_m$, n = 2 to 3 and m = 0 to 2; and the ions with masses 94, 122 and 150 are $O_2^-(CO_2)(H_2O)(N_2)_m$, m = 0 to 2. In Figure 3, an elevated $CO_2$ concentration increased the relative abundance of the $O_2^-(CO_2)(H_2O)(N_2)_m$ ions. For both cases, methyl salicylate was ionized by producing $O_2^-(MS)(N_2)_m$ ions at masses 184, 212, 240 and 268 and proton abstracted ions at mass 151. A comparison of the relative amplitudes in Figure 2 shows that methyl salicylate was ionized by reaction with the $O_2^-(CO_2)(H_2O)(N_2)_m$ reactant ions, but not the $CO_3^-(H_2O)_n(N_2)_m$ reactant ions.

Figure 4 compares the negative reactant ions when purified air versus argon was used for the drift gas. Purified air was used for the carrier and sample gases in both cases. Since the 13X scrubbers were activated at 300 °C, the extent of water clustering was reduced and the ions with masses 50 ($O_2^-(H_2O)$), 82 ($O_4^-(H_2O)$) and 76 ($O_2^-(CO_2)$) were much stronger. The water clusters at masses 68 ($O_2^-(H_2O)_2$), 94 ($O_2^-(CO_2)(H_2O)$) and 100 ($O_4^-(H_2O)_2$) increased when the drift gas was switched to argon. Two possible explanations are possible for this shift: (1) the argon drift gas was wetter than the purified air and (2) argon is less likely to collisionally dissociate the ion clusters as they drifted through the drift tube. Since the first possibility is supported by a higher reading on the hygrometer when argon was used as the drift gas and the second possibility is consistent with increased cluster stabilities which might accompany the lower drift fields used (to eliminate gas breakdown) to collect the argon results, the experimental evidence is inconclusive.

More significantly (and the reason why the data were collected), the results of Figure 4 show that the nitrogen clusters (e.g., masses 78, 96, 110 and 138) were observed independent of whether the drift gas was purified air or argon. Since an unidirectional flow scheme was used for the carrier and drift gases, nitrogen should not have built up in the argon drift gas. This means that the nitrogen clusters most likely formed in the reactor and not in the drift tube or the molecular beam issuing from the pinhole.

Instead of using purified air for the sample gas, Figure 5 shows the negative reactant ions when sampling 100% $CO_2$ with the membrane inlet. Unlike the results of Figures 2 and 4, the major reactant ions were $O_2^-(CO_2)(H_2O)_n$, masses 76 and 94, when purified air was used for the carrier and drift gases and $CO_3^-(Ar)_n$, masses 60, 100 and 140, when argon was used for the carrier and drift gases. As expected $CO_2$, made a significant contribution to the composition of the ions. The appearance of argon clusters of $CO_3^-$ was surprising. It demonstrated that ligands do not have to be polar before they can cluster with an ion. The $CO_3^-(Ar)_n$ ions were persistent even when purified air or argon was used for the sample gas. This latter result demonstrates that the reactions leading to the $CO_3^-(Ar)_n$ ions are strongly exothermic.

Figure 6 shows the effects of adding purified air to the argon drift gas of Figure 5. As the purified air concentration increased, the amplitude of the $CO_3^-(Ar)_n$ ions decreased. With the introduction of as little as 1.1% purified air into the argon, the $O_2^-(CO_2)(H_2O)_n$ ions at masses 76 and 94 were the major reactant ions. While there was an ion at mass 116, corresponding to $O_2^-(CO_2)(Ar)$, in the 1.1% data, this ion disappeared when the purified air concentration rose to 6.3%.

Figure 7 shows mass spectra for the negative reactant ions and methyl salicylate when the UV photoionization flashlamp was used for ionization. Like Figures 2 and 3, the methyl salicylate was introduced by challenging the membrane inlet of the IMS cell with 0.02-0.03 mg/m$^3$ methyl salicylate in purified air. The photoionization flashlamp produced only $CO_3^-(Ac)_x(N_2)_m$ ions at masses 60, 88, 116, 118 and 146 where x = 0 to 1 and m = 0 to 3. The acetone adduct (Ac) was present because 58 ppm acetone was in the reactor when the data were collected. Inconsistent with the results of Figures 2 and 3, the methyl salicylate was not ionized using these reactant ions.

To explore the lack of response to methyl salicylate, data were collected with a combination reactor where the ions produced by a radioactive source were irradiated by the UV photoionization flashlamp. Figure 8 shows the results when the membrane inlet was challenged with 0.02-0.03 mg/m$^3$ methyl salicylate. The top spectrum was collected with the flashlamp off. Similar to Figure 2, the methyl salicylate was ionized by forming $O_2^-(MS)(N_2)_m$ product ions. The bottom spectrum was collected with the flashlamp on. The $CO_3^-(Ac)(N_2)_m$ reactant ions reappeared, and the methyl salicylate was no longer ionized. Apparently the photoionization flashlamp altered the composition of the reactant ions sufficiently to prevent the ionization of methyl salicylate. This result was independent of the flash rate used for the flashlamp.

## DISCUSSION

Carr has shown that the negative reactant ions in IMS are primarily $O_2^-(H_2O)_n$ when purified air is used for the carrier and drift gases.[18] In the presence of $CO_2$, Mohnen observed $CO_4^-$ and its hydrate resulting from the following reactions.[19]

$$O_2^- + CO_2 \rightleftharpoons O_2^-(CO_2) \overset{+H_2O}{\rightleftharpoons} O_2^-(CO_2)(H_2O)$$

These ions appear in the mass spectrum at masses 76 and 94 and are noted in Figures 3 and 5. Hayhurst et al. found that the $CO_4^-$ ions become important when the $CO_2$ concentration increases from about 2 ppm to 100 ppm.[3] Ab initio calculations show that the $CO_4^-$ ion is a $\pi$-$\pi^*$ complex with oxygen bridging a C+O bond in $CO_2$ and that 0.8 ± 0.08 eV is required to dissociate $O_2^-(CO_2)$ into $O_2^-$ and $CO_2$.[20,21] Since Fehsenfeld and Ferguson found that[22]

$$O_2^-(H_2O) + CO_2 \rightleftharpoons CO_4^- + H_2O \qquad -\Delta G^\circ_{296} = 2.1 \text{ kJ/mol}$$

$$CO_4^-(H_2O) + H_2O \rightleftharpoons O_2^-(H_2O)_2 + CO_2 \qquad -\Delta G^\circ_{296} = 6.7 \text{ kJ/mol}$$

the appearance of $CO_4^-$ is more favorable in the presence of reduced water and/or elevated $CO_2$ concentrations.[23]

When the $O_2^-(H_2O)_n$ or $CO_4^-(H_2O)_n$ ions are formed under atmospheric pressure conditions, they may also contain nitrogen ($N_2$) adducts. This is evidenced by a series of ions separated by 28 mass units in the mass spectrum. Because CO also has a mass of 28 and is a more polar molecule than nitrogen, it can also contribute to the 28 mass unit differences in the mass spectrum. For the present data, however, there are several arguments against the CO assignment. First, CO was not intentionally introduced into the IMS; second, nitrogen was the major component when purified air was used for the carrier and drift gases; and third, the nitrogen adducts could be correlated with the presence of purified air in the reactor (see a companion paper given at this workshop).

When using a drift temperature of 50 °C, Spangler, et al. identified the presence of nitrogen adducts in both the positive and negative ion spectra using IMS/MS.[4,24] At the risk of oversimplifying the situation, as many as 3 nitrogens were attached to the positive ion (e.g., $H_3O^+(H_2O)_4$) and as many as 2 nitrogens were attached to the negative ion (e.g., $O_2^-(CO_2)$). This difference suggests that the affinity of the ion for the nitrogen adduct is greater when the ion contains a positive charge. If the attraction is due to an ion-induced dipole interaction, this means that a positive charge induces a stronger dipole in the adduct than a negative charge. While other factors relating to the distribution of the charge on the ion may also be important, this result is consistent with the fact that opposite charges attract and the positive nuclear charge is shielded by valence electrons.

The mechanism whereby $CO_3^-$ is formed in IMS is less understood than $CO_4^-$. For purposes of

discussion, five possible mechanisms are proposed. The first two were first mentioned by Fehsenfeld and Ferguson who proposed that $O^-$ is produced in the gas phase by dissociative attachment of electrons to $O_2$ or by ion pair production.[22,25] That is[26,27]

$$\beta^-(67\ keV) + O_2 \rightarrow O + O^-$$

$$O^- + n(H_2O) \rightleftharpoons O^-(H_2O)_n$$

$$O^-(H_2O)_n + CO_2 \rightleftharpoons CO_3^-(H_2O)_m + (n\text{-}m)H_2O$$

or

$$\beta^-(67\ keV) + O_2 \rightarrow O^+ + O^-$$

$$O^- + n(H_2O) \rightleftharpoons O^-(H_2O)_n$$

$$O^-(H_2O)_n + CO_2 \rightleftharpoons CO_3^-(H_2O)_m + (n\text{-}m)H_2O$$

where $\beta^-(67\ keV)$ is the beta particle emitted by the $^{63}Ni$ radioactive source. The second three depend on the presence of metastable nitrogen ($N_2^*$) originating from the Vegard-Kaplan $A\ ^3\Sigma_u^+ - X^1\Sigma_g^+$ transition with 6.3 eV of energy.[28,29]

$$O_2 + N_2^* \rightarrow 2O + N_2 + 1.1\ eV$$

$$e^-(thermal) + O \rightarrow O^-$$

$$O^- + n(H_2O) \rightleftharpoons O^-(H_2O)_n$$

$$O^-(H_2O)_n + CO_2 \rightleftharpoons CO_3^-(H_2O)_m + (n\text{-}m)H_2O$$

or

$$O_2^- + N_2^* \rightarrow O + O^- + N_2 + 2.2\ eV$$

$$O^- + n(H_2O) \rightleftharpoons O^-(H_2O)_n$$

$$O^-(H_2O)_n + CO_2 \rightleftharpoons CO_3^-(H_2O)_m + (n\text{-}m)H_2O$$

and

$$CO_4^- + N_2^* \rightarrow CO_3^- + O + N_2 + 3.4\ eV$$

$$CO_3^- + n(H_2O) \rightleftharpoons CO_3^-(H_2O)_n$$

One source for the metastable nitrogen is recombination of $N_2^+$ which serves as a precursor ion to the formation of the positive reactant ions .[30]

The dissociative attachment and ion pair production mechanisms for $O^-$ need no additional energy other than that provided by the $\beta^-$-particle. Once the $O^-$ is formed, it reacts readily with $CO_2$ with an exothermicity of 52 kcal/mol.[31,32,33] If the $O^-$ should be clustered with water, the reaction is still exothermic since the enthalpy

of hydration is only 30 kcal/mol.[31] Because of the excess energy, the reactions proceed to completion and yield less $CO_3^-$ when the oxygen content of the carrier and drift gases is reduced. This latter observation contradicts the findings of Carr who observed an increase in $CO_3^-$ ions when the drift gas was changed from air to nitrogen at 210 °C.[18] Consequently, doubt is cast on the role which dissociative attachment and ion pair production play in the formation of $CO_3^-$.

During their studies on the negative reactant ions between 25 and 55 °C, Hayhurst, Watts and Wilders did not detect $O^-$ ions.[3] On the other hand, they were able to identify the presence of $CO_3^-$ ions using isotope dilution techniques. Using IMS data, they also found that "in a dry system, increasing the $CO_2$ concentration decreases the amount of $CO_3^-$ formed; in a wet system, the $CO_2$ concentration has no marked effect on $CO_3^-$ production." This water effect shows features similar to those observed by Fehsenfeld and Ferguson when they studied $CO_4^-$ (see above).[22] Unlike Hayhurst, Watts and Wilders, however, Fehsenfeld and Ferguson noted an increased yield for $CO_4^-$ the concentration of $CO_2$ was increased.

The involvement of metastable nitrogen in the formation of $CO_3^-$ has not yet been hypothesized in the open literature. On the other hand, it is consistent with the experimental results for argon where a much greater tendency towards the formation of $CO_3^-$ was observed. Metastable argon has an excitation energy of 11.6 eV.[28] In the presence of trace concentrations of oxygen and carbon dioxide, the following reactions can occur.

$$O_2 + Ar^* \rightarrow 2O + Ar + 6.4\ eV$$

$$e^-(thermal) + O \rightarrow O^-$$

$$O^- + n(H_2O) \rightleftharpoons O^-(H_2O)_n$$

$$O^-(H_2O)_n + CO_2 \rightleftharpoons CO_3^-(H_2O)_m + (n\text{-}m)H_2O$$

or

$$O_2^- + Ar^* \rightarrow O + O^- + Ar + 7.5\ eV$$

$$O^- + n(H_2O) \rightleftharpoons O^-(H_2O)_n$$

$$O^-(H_2O)_n + CO_2 \rightleftharpoons CO_3^-(H_2O)_m + (n\text{-}m)H_2O$$

and

$$CO_4^- + Ar^* \rightarrow CO_3^- + O + Ar + 8.7\ eV$$

$$CO_3^- + n(H_2O) \rightleftharpoons CO_3^-(H_2O)_n$$

These are the same reactions proposed with nitrogen, except Ar* replaces $N_2$* in the equations. Because the excitation energy for metastable argon is greater than metastable nitrogen, the reactions are more exothermic. Hence less $CO_2$ sample gas is needed to saturate the $CO_3^-$ response when argon is used for the carrier and drift gases than when purified air is used for the carrier and drift gases. Except to say that metastable neutral species play a role in forming $CO_3^-$, it is not yet possible to identify with confidence the set of reactions most responsible for the ionization. Because of its high energy, metastable argon may participate in all the reactions. Because its energy is low, metastable nitrogen may not participate as freely. This should become more so if cluster growth occurs in the presence of water.

In the presence of UV radiation, ozone is easily generated because of the large cross section offered by the Schumann-Runge system (complete absorption below 175.9 nm) of oxygen and the low heat of formation for ozone (34.1 kcal/mol).[34,35] Watts in his compilation of kinetic data for IMS noted that a pathway to $CO_3^-$ from ozone might be[36]

$$O_2^-(H_2O)_n + O_3 \rightarrow O_3^-(H_2O)_{n-1} + O_2 + H_2O$$

$$O_3^-(H_2O)_n + CO_2 \rightarrow CO_3^-(H_2O)_{n-1} + H_2O + O_2$$

If this proposal is correct, it would seem that the results of Figures 7 and 8 can be explained on the basis that photoelectrons generated by the flashlamp are captured by ozone which then react with $CO_2$ to form $CO_3^-$. The reaction scheme is consistent with the fact that the results in Figures 7 and 8 are independent of the flash rate used for the flashlamp.

The inability to ionize methyl salicylate with $CO_3^-(H_2O)_n(N_2)_m$ reactant ions is related to the distribution of the charge on the ion. Ab initio calculations show that the ground state for $CO_3^-$ ion is a $^2B_1$ state with $C_{2v}$ symmetry and an OCO angle of 131.36°.[37] The electronic configuration can be viewed as a resonating structure which spreads the ionic charge over the three legs of the ion. When the ion attacks a methyl salicylate molecule, the strength of the induced dipole interaction is weakened by the delocalized ionic charge. This causes the ion/molecule complex to be unstable towards dissociation with a lifetime short compared to the drift time for the ion. This is unlike the reaction of methyl salicylate with the dioxygen anion, $O_2^-$, which does form a stable $(M+O_2)^-$ complex.

## CONCLUSIONS

The effects of $CO_2$ on the negative reactant ions in IMS is to form ion clusters of $CO_4^-$ and $CO_3^-$. The $CO_4^-$ ions are formed by direct association, but the $CO_3^-$ ions require additional energy. This additional energy can be provided by either neutral metastable gas molecules or UV radiation. When metastable nitrogen is involved in the reactions, the reactions are mildly thermoneutral making the yield of $CO_3^-$ is strongly temperature dependent. When metastable argon or UV irradiation are involved in the reactions, excess energy is generated and the ion/molecule reactions are saturated towards $CO_3^-$. Methyl salicylate can be ionized using $CO_4^-$ reactant ions, but not $CO_3^-$ reactant ions.

## REFERENCES

1. Spangler, G.E. and Collins, C.I. Reactant Ions in Negative Ion Plasma Chromatography. *Anal. Chem.* **47**, 393-402 (1975).

2. Rokushika, S., Hatano, H. and Hill, H.H., Jr. Ion Mobility Spectrometry in Carbon Dioxide. *Anal. Chem.* **58**, 361-365 (1986).

3. Hayhurst, C.J., Watts, P. and Wilders, A. Studies on Gas-Phase Negative Ion-Molecule Reactions of Relevance to Ion Mobility Spectrometry: Mass Analysis and Ion Identification of the Negative Reactant Ion Peak in "Clean" Air. *Int. J. Mass Spectrom. Ion Proc.* **121**, 127-139 (1992).

4. Spangler, G.E. and Carrico, J.P. Membrane Inlet for Ion Mobility Spectrometry (Plasma Chromatography). *Int. J. Mass Spectrom. Ion Phys.* **52**, 267-287 (1983).

5. Nowak, D.M. Mobility and Molecular Ions of Dimethyl Methyl Phosphonate, Methyl Salicylate, and Acetone. Technical Report ARCSL-TR-83056, U.S. Army Armament R&D Command, Chemical Systems Laboratory, Aberdeen Proving Ground, MD, June 1983.

6. Spangler, G.E. and Roehl, J.E. Nonradioactive Source Development for the XM22 Automatic Chemical Agent Alarm and Auxiliary Equipment. Technical Report on Contract DAAA15-90-C-0030, U.S. Army Edgewood Research, Development and Engineering Center, Aberdeen Proving Ground, MD 21010 by Environmental Technologies Group, Inc., 1400 Taylor Avenue, Baltimore 21284-9840, December 1992.

7. Extrel Corporation, 240 Alpha Drive, Box 11512, Pittsburgh, PA 15238.

8. Spangler, G.E. Membrane Interface for Ion Mobility Detector Cells. U.S. Patent 4,311,699, The Bendix Corporation, Southfield, MI, January 1982.

9. Browning, D.R., Sima, G.R., Jr., Schmidt, J.C. and Sickenberger, D.W. One Piece Ion Accelerator for Ion Mobility Detector Cells. U.S. Patent 4,390,784, The Bendix Corporation, Southfield, MI, June 1983.

10. New England Nuclear, 549 Albany Street, Boston, MA 02118.

11. EG&G Electro-Optics, 35 Congress Street, Salem, MA 01970.

12. Interconics, Buckbee Mears, Inc., 245 E. 6th St., St. Paul, MN 55101.

13. Matheson Gas Products, 30 Seaview Dr., P.O. Box 1587, Secaucus, NJ 07096.

14. Balston, Inc., 260 Neck Rd., Haverhill, MA 01835.

15. W.R. Grace & Co., Davison Chemical Division, P.O. Box 2117, Baltimore, MD 21203.

16. Ametek, 455 Corporate Blvd., Pencador Corporate Ctr., Newark, DE 19702.

17. Airgas, 100 Matsonford Road, Suite 550, Radnor, PA 19087.

18. Carr, T.W. Comparison of the Negative Reactant Ions Formed in the Plasma Chromatograph by Nitrogen, Air, and Sulfur Hexafluoride as the Drift Gas with Air as the Carrier Gas. *Anal. Chem.* **51**, 705-711 (1979).

19. Mohnen, V.A. *Pure Appl. Geophys.* **100**, 123 (1972).

20. Hiraoka, K. and Yamabe, S. Formation of the Chelate Bonds in the Cluster $O_2^-(CO_2)_n$, $CO_3^-(CO_2)_n$ and $NO_2^-(CO_2)_n$. *J. Chem. Phys.* **97**, 643-650 (1992).

21. Pack, J.L. and Phelps, A.V. Electron Attachment and Detachment. II. Mixtures of $O_2$ and $CO_2$ and of $O_2$ and $H_2O$. *J. Chem. Phys.* **45**, 4316-4329 (1966).

22. Fehsenfeld, F.C. and Ferguson, E.E. Laboratory Studies of Negative Ion Reactions with Atmospheric Trace Constituents. *J. Chem. Phys.* **61**, 3181-3193 (1974).

23. Ellis, H.W., Pai, R.Y., Gatland, I.R., McDaniel, E.W., Wernlund, R. and Cohen, M.J. Ion Identity and Transport Properties in $CO_2$ Over a Wide Pressure Range. *J. Chem. Phys.* **64**, 3935-3941 (1976).

24. Kim, S.H. and Spangler, G.E. Ion Mobility Spectrometry/Mass Spectrometry (IMS/MS) of Two Structurally Different Ions Having Identical Ion Mass. *Anal. Chem.* **57**, 567-569 (1985).

25. Siegel, M.W. and Fite, W.L. Terminal Ions in Weak Atmospheric Pressure Plasmas. Application of Atmospheric Pressure Ionization to Trace Impurity Analysis in Gases. *J. Phys. Chem.* **80**, 2871-2881 (1976).

26. Chase, M.W., Jr., Davies, C.A., Downey, J.R., Jr., Frurip, D.J., McDonald, R.A. and Syverud, A.N. JANAF Thermochemical Tables, Third Edition. *J. Phys. Chem. Ref. Data* **14**(Suppl. 1), 1-1856 (1985).

27. Rosenstock, H.M., Draxl, K., Steiner, B.W. and Herron, J.T. Energetics of Gaseous Ions. *J. Phys. Chem. Ref. Data* **6**(Suppl. 1), 1-783 (1977).

28. Littlewood, A.B. Gas Chromatography: Principles, Techniques, and Applications. Academic Press, NY, 1970.

29. Herzberg, G. Molecular Spectra and Molecular Structure: I. Spectra of Diatomic Molecules. Van Nostrand Reinhold Company, NY, 1950.

30. Carroll, D.I., Dzidic, I., Stillwell, R.N. and Horning, E.C. Identification of Positive Reactant Ions Observed for Nitrogen Carrier Gas in Plasma Chromatograph Mobility Studies. *Anal. Chem.* **47**, 1956-1959 (1975).

31. Keesee, R.G. and Castleman, A.W., Jr. Thermochemical Data on Gas-Phase Ion-Molecule Association and Clustering Reactions. *J. Phys. Chem. Ref. Data* **15**(3), 1011-1071 (1986).

32. Moruzzi, J.L. and Phelps, A.V. Survey of Negative-Ion-Molecule Reactions in $O_2$, $CO_2$, $H_2O$, CO and Mixtures of These Gases at High Pressure. *J. Chem. Phys.* **45**, 4617-4627 (1966).

33. Bohme, D.K., Dunkin, D.B., Fehsenfeld, F.C. and Ferguson, E.E. Flowing Afterglow Studies of Ion-Molecule Association Reactions. *J. Chem. Phys.* **51**, 863-872 (1969).

34. Handbook of Optics, W.G. Driscoll, W. Vaughan, Eds. McGraw Hill, NY, 1978.

35. CRC Handbook of Chemistry and Physics, D.R. Lide, Ed. CRC Press, Boca Raton, FL, 1994.

36. Watts, P. Studies on Gas-Phase Negative Ion-Molecule Reactions of Relevance to Ion Mobility Spectrometry: Kinetic Modeling of the Reactions Occurring in "Clean" Air". *Int. J. Mass Spectrom. Ion Proc.* **121**, 141-158 (1992).

37. So, S.P. Ground Electronic State and Geometry of the $CO_3^-$ Radical Anion. *J. Chem. Phys., F. Trans. II* **72**, 646-650 (1976).

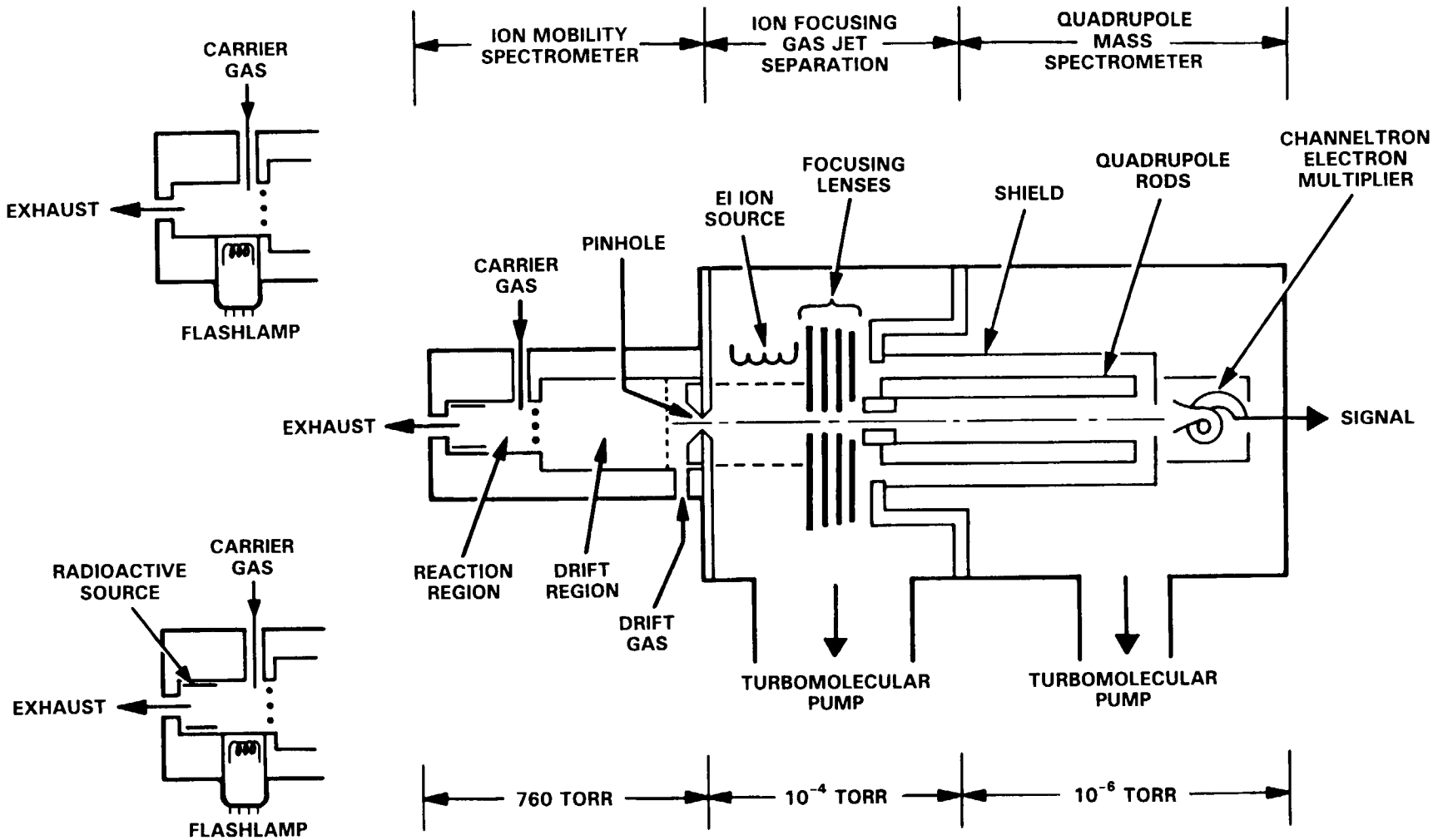


**Figure 1. Functional Diagram for the Ion Mobility Spectrometer/Mass Spectrometer System. The** Photoionization Reactor (top) and the Photoionization Reactor Equipped with a Radioactive Source (bottom) Are Shown on the Left.

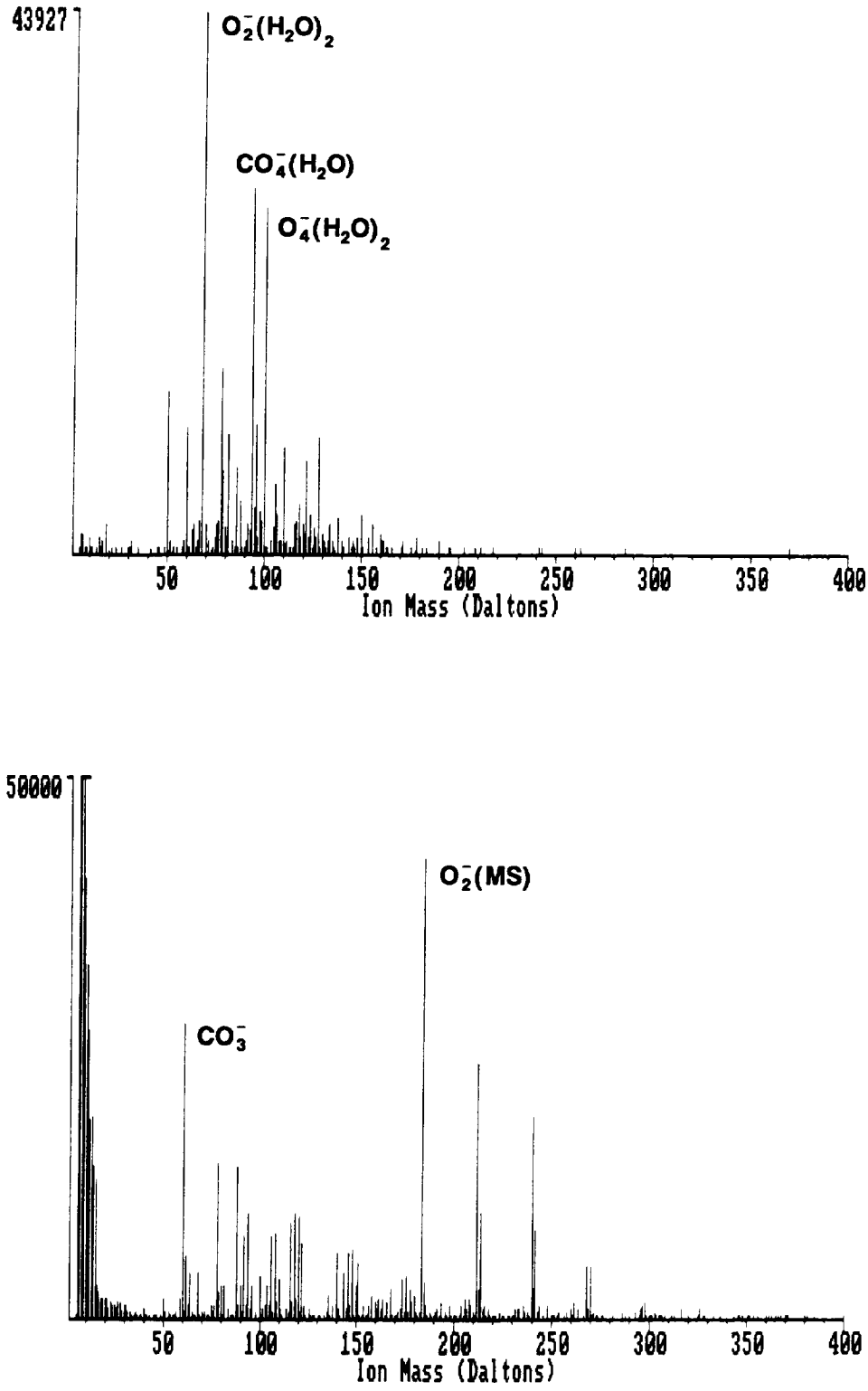


**Figure 2. Negative Reactant Ions (top) and the Negative Ionization of Methyl Salicylate (bottom) using a** 13X Scrubber Immediately after Reactivation at 200 °C.

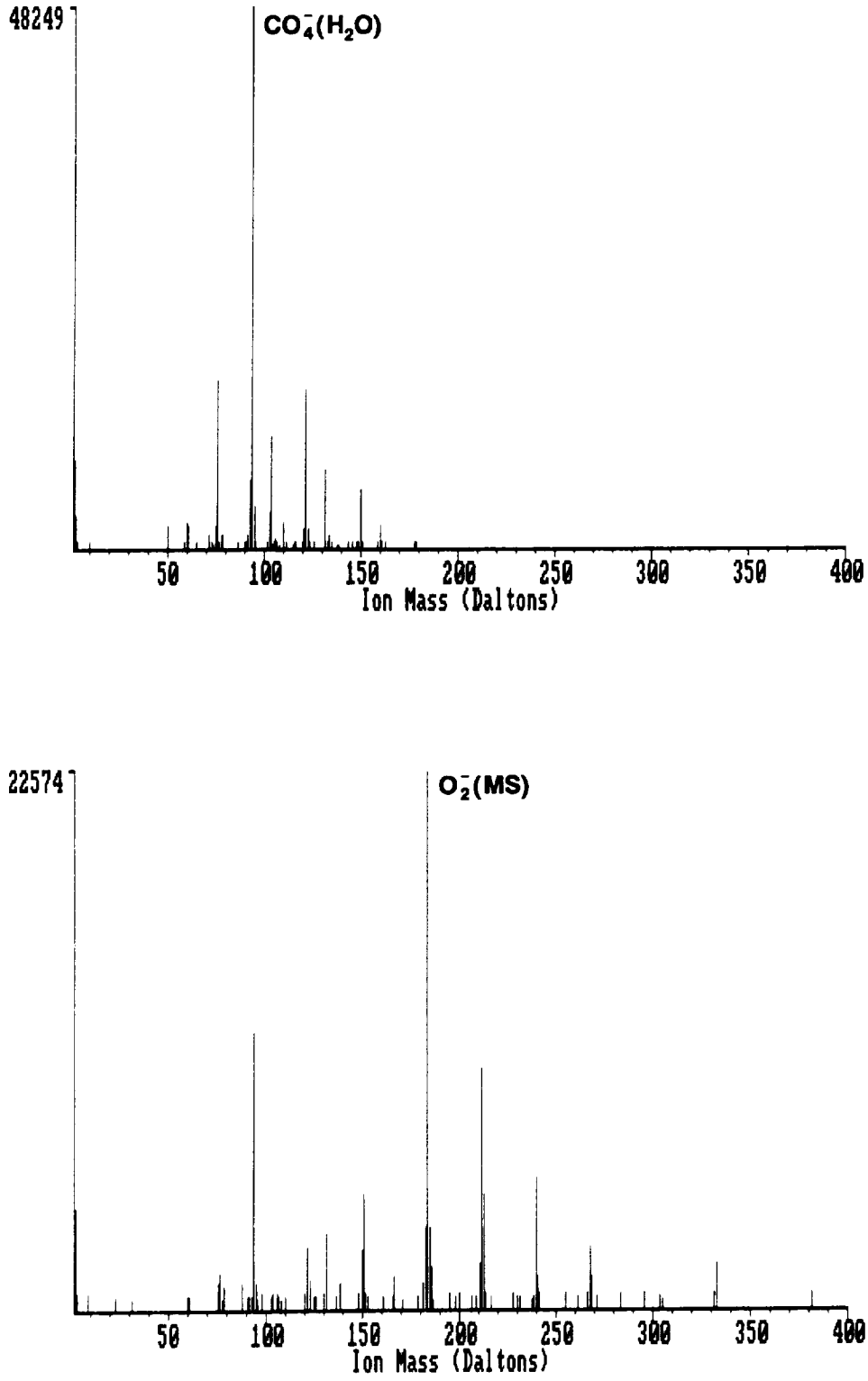


**Figure 3. Negative Reactant Ions (top) and the Negative Ionization of Methyl Salicylate (bottom) using an** Aged 13X Scrubber Several Hours after Reactivation at 200 °C.

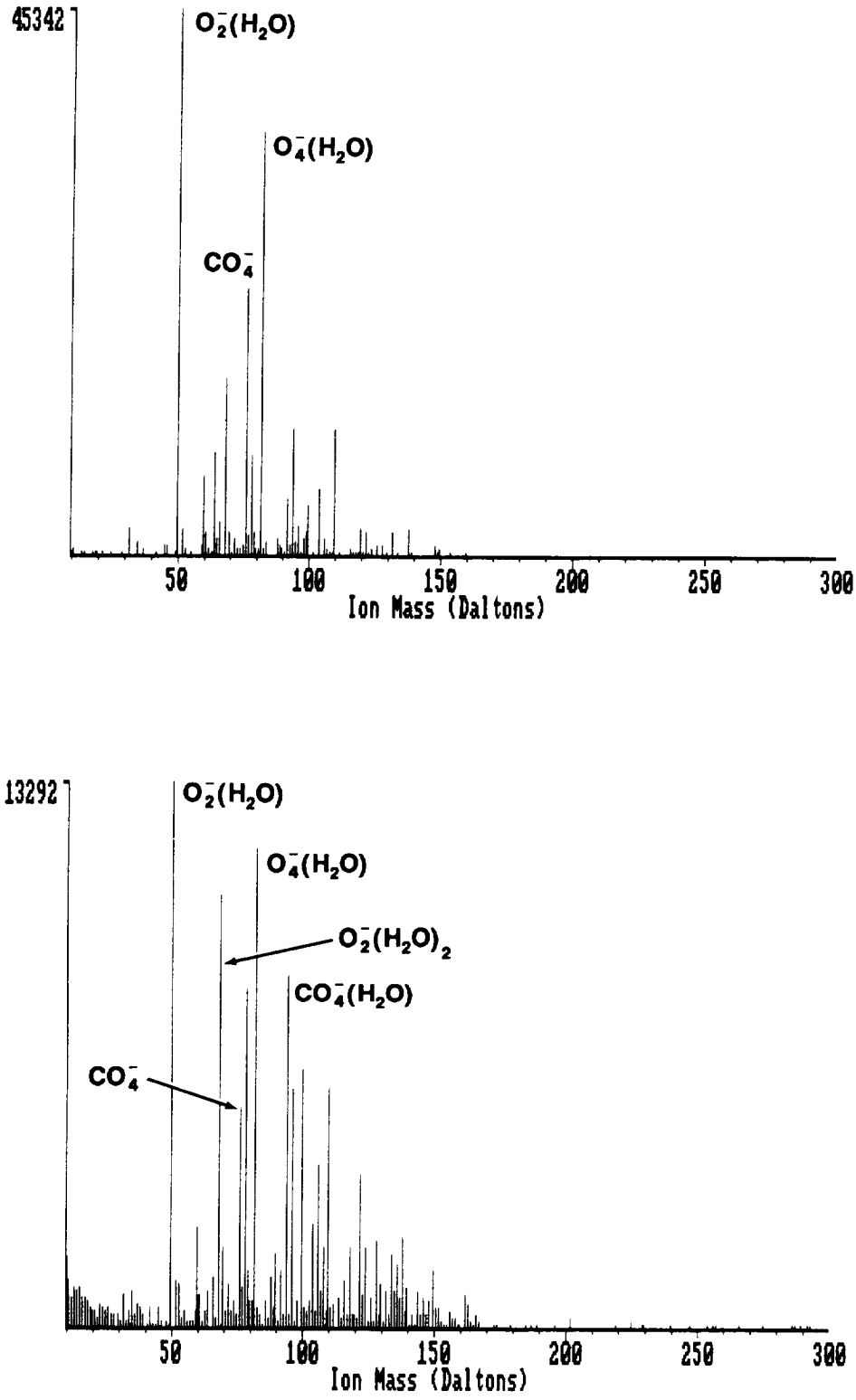


**Figure 4. Negative Reactant Ions Using Purified Air (top) and Argon (bottom) for the Drift Gas. Purified Air** was used for the Carrier and Sample Gases.

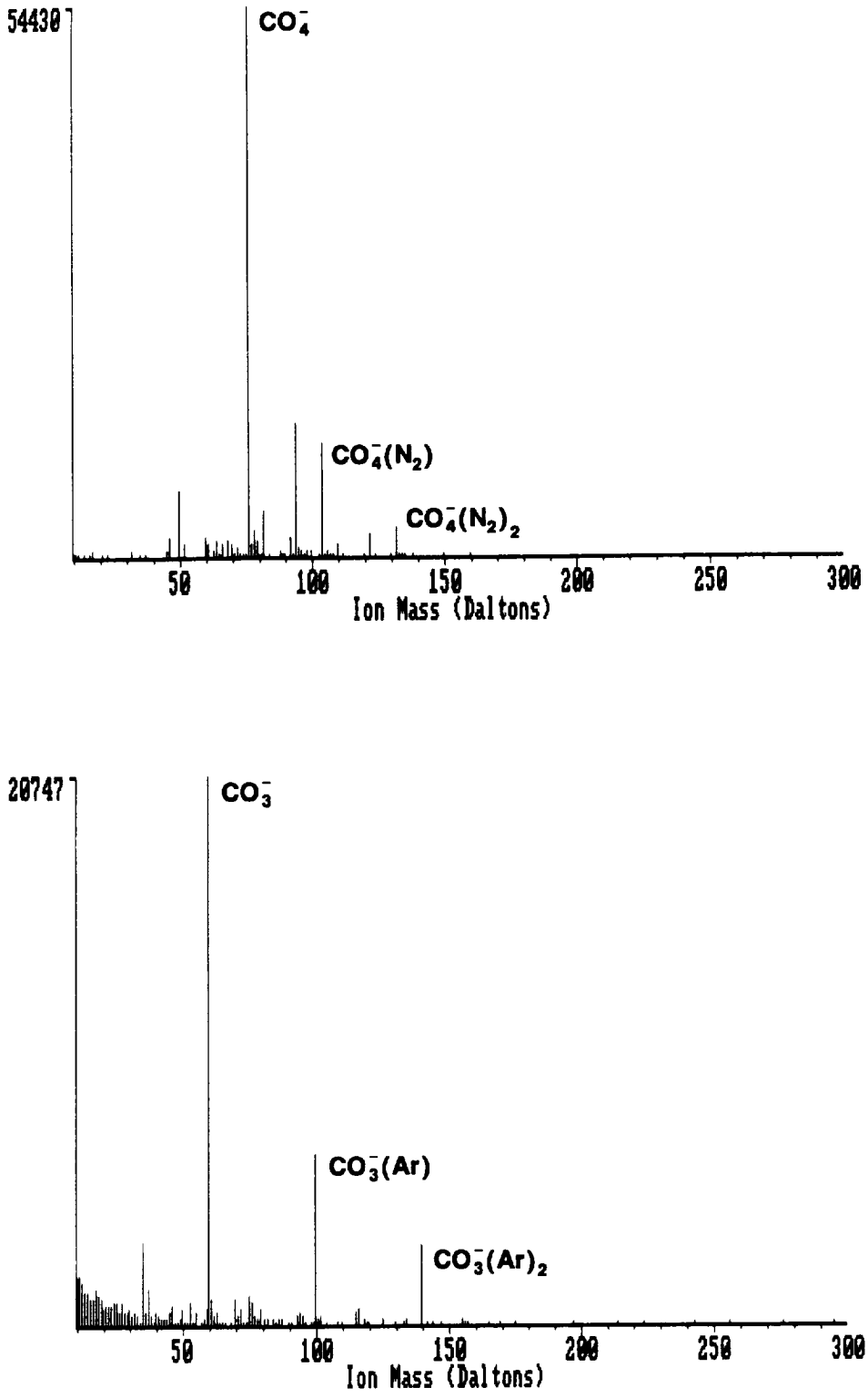


**Figure 5. Negative Reactant Ions Using Purified Air (top) and Argon (bottom) for the Carrier and Drift Gases.** The Membrane Inlet was challenged with $CO_2$.

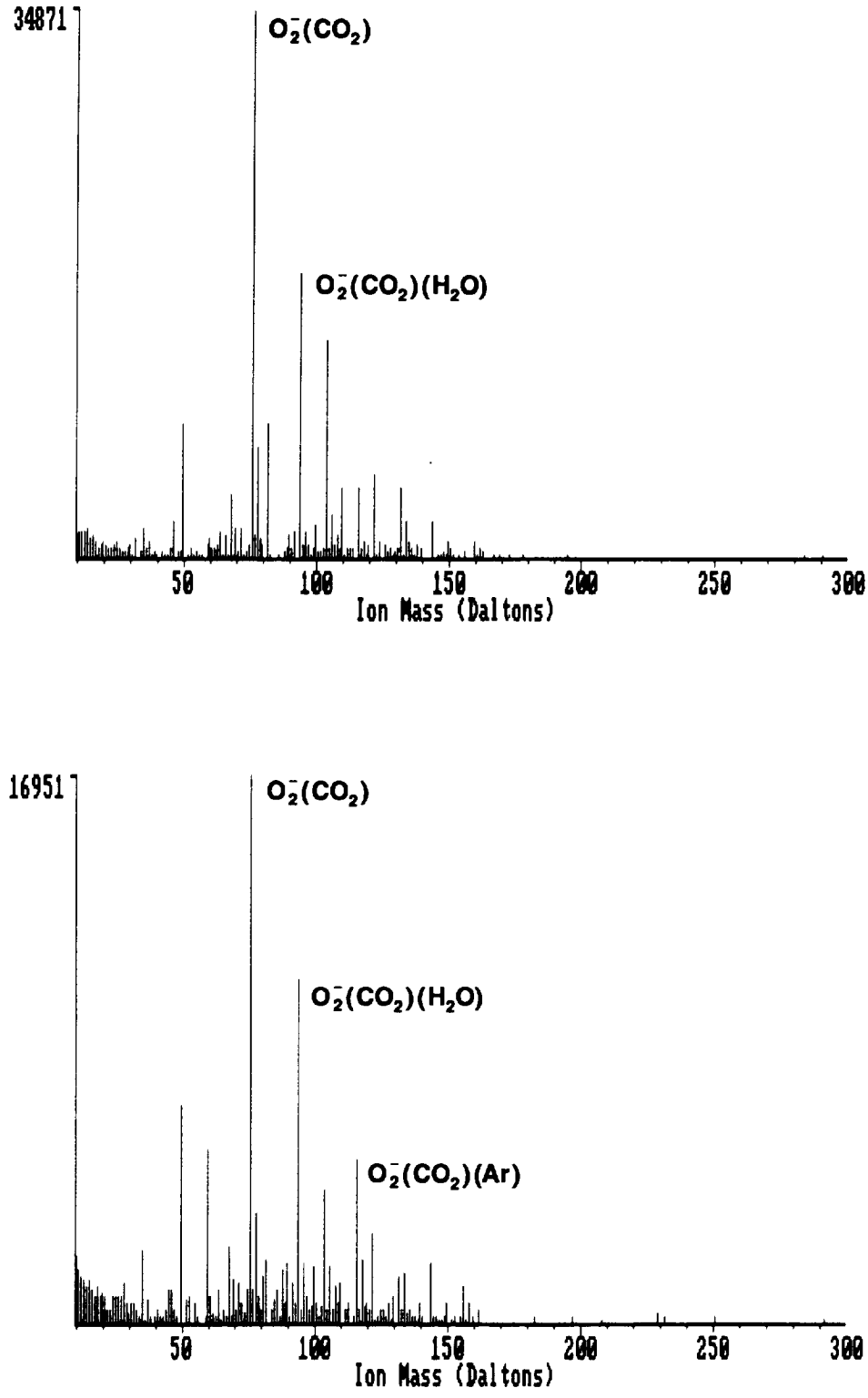


**Figure 6. Negative Reactant Ions Using Argon for the Carrier and Drift Gases and $CO_2$ for the Sample Gas.** 1.1% Purified Air (bottom) and 6.3% Purified Air (top) was introduced into the Argon Drift Gas.

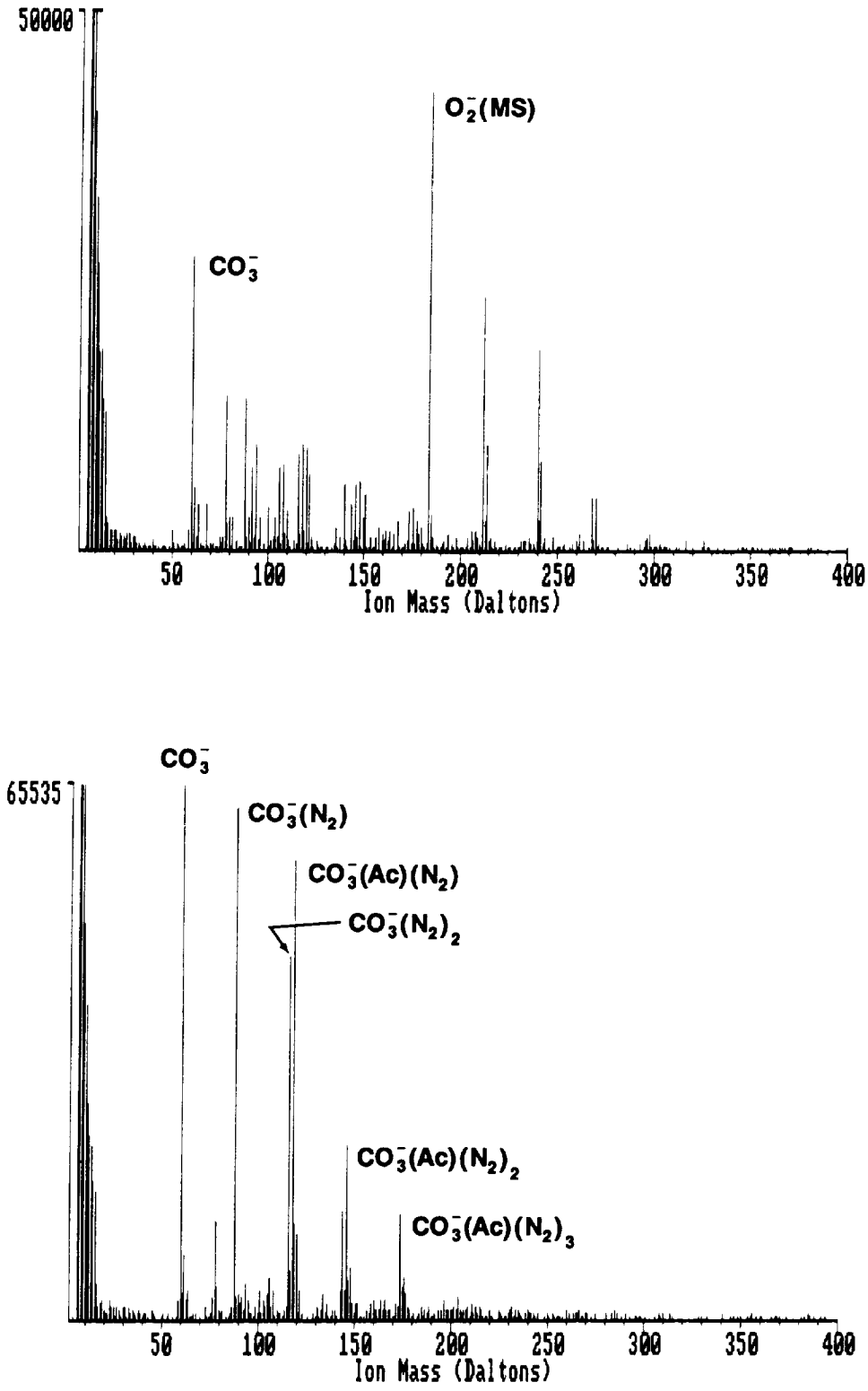


**Figure 8. Negative Ionization of Methyl Salicylate using a Radioactive Source with (bottom) and without** (top) the Product Ions being Irradiated with UV Radiation from the Photoionization Source.